On Theoretical Broadband Shock-Associated Noise Near-Field Cross-Spectra

Steven A. E. Miller
The National Aeronautics and Space Administration
NASA Langley Research Center
Aeroacoustics Branch

AIAA Aeroacoustics Conference 2015
June 22nd – 26th 2015

Acknowledgements

- NASA Advanced Air Vehicles Program
  Commercial Supersonic Technology Project
- Alessandro Savarese of The Airbus Group
- James Bridges of NASA Glenn Research Center
- Krishnamurthy Viswanathan of The Boeing Company
- Many previous curious researchers

Introduction

Aerospace Flight Vehicles

Need for first principles mathematical theory to predict
cross-spectra at observers and on the flight vehicle airframe

Image Credit: NASA/Boeing
Website: NASA.gov

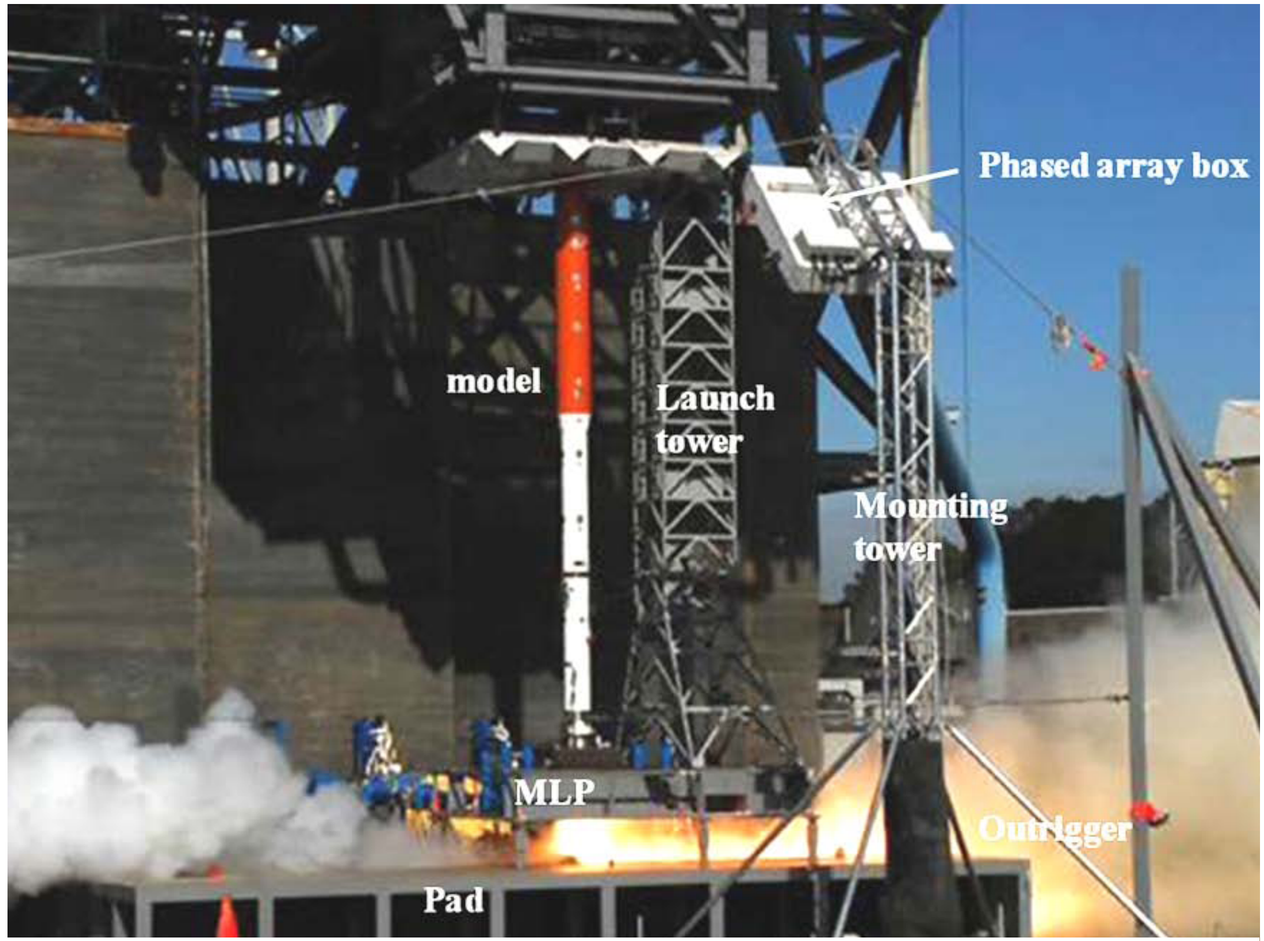

Panda, J. and Mosher, R., `Microphone Phased Array to Identify Liftoff Noise Sources in Model Scale Tests,' Journal of Spacecraft and Rockets, Vol. 50, No. 5., 2013. DOI: 10.2514/1.A32433

Modeling Goals

- Predict auto-spectra and cross-spectra of BBSAN
- Capture acoustic near-field and far-field effects
- Include the flight vehicle Mach number
- Desire simple closed-form equation
- Evaluate quickly
- Validate for
  - Multiple jet Mach numbers and temperature ratios
  - Far- and near-field auto-spectra and coherence
- Gain insight into the physical process

Mathematical Approach

Mathematical Overview

- Governing equations are Navier-Stokes
- Derive Lighthill analogy for pressure with ambient meanflow, and solve in most general fashion
- Form two-point correlation, subsequent cross-power spectral density, simplify, obtain "Cross-Power Spectral Density Acoustic Analogy"
- Model $T_{ij}T_{lm}$ for BBSAN source, simplify, and obtain model dependent on turbulent statistics
- Model turbulent statistics
- Reduce model equation to simple double summation using reasonable assumptions

Forming a Two-Point Pressure Correlation

Form an acoustic analogy from the Navier-Stokes equations

Solving and expanding the source terms

$$p(\boldsymbol{x},t) = \frac{1}{4\pi}\int_{-\infty}^{\infty}\int_{-\infty}^{\infty}\int_{-\infty}^{\infty}\left\{\frac{r_i r_j}{r^2}\left[\frac{\ddot{T}_{ij}}{c_\infty^2 r} + \frac{3(1-M_\infty^2)\dot{T}_{ij}}{c_\infty r^2} + \frac{3(1-M_\infty^2)^2 T_{ij}}{r^3}\right]\right.$$

$$\left. -\frac{2r_i M_{\infty,j}}{r}\left[\frac{2\dot{T}_{ij}}{c_\infty r^2} + \frac{3(1-M_\infty)^2 T_{ij}}{r^3}\right] - \delta_{ij}\left[\frac{\dot{T}_{ij}}{c_\infty r^2} + \frac{(1-M_\infty^2)T_{ij}}{r^3}\right] + 2M_{\infty,i}M_{\infty,j}\frac{T_{ij}}{r^3}\right\} d\boldsymbol{\eta}$$

Finding the two-point correlation of the pressure

$$\overline{p(\boldsymbol{x},t)\,p(\boldsymbol{x}',t')} = \frac{1}{16\pi^2}\int_{-\infty}^{\infty}\cdots\int_{-\infty}^{\infty}\left(A_1 + A_2 + A_3 + A_4\right) d\boldsymbol{\eta}'\,d\boldsymbol{\eta}$$

where

$$A_1 = \frac{r_i r_j r_l' r_m'}{r^2 r'^2}\overline{\left[\frac{\ddot{T}_{ij}}{c_\infty^2 r} + \frac{3(1-M_\infty^2)\dot{T}_{ij}}{c_\infty r^2} + \frac{3(1-M_\infty^2)^2 T_{ij}}{r^3}\right]\left[\frac{\ddot{T}'_{lm}}{c_\infty^2 r'} + \frac{3(1-M_\infty^2)\dot{T}'_{lm}}{c_\infty r'^2} + \frac{3(1-M_\infty^2)^2 T'_{lm}}{r'^3}\right]}$$

$$-\frac{2r_i r_j}{rr}\frac{r_l' M_{\infty,m}}{r'}\overline{\left[\frac{\ddot{T}_{ij}}{c_\infty^2 r} + \frac{3(1-M_\infty^2)\dot{T}_{ij}}{c_\infty r^2} + \frac{3(1-M_\infty^2)^2 T_{ij}}{r^3}\right]\left[\frac{2\dot{T}'_{lm}}{c_\infty r'^2} + \frac{3(1-M_\infty)^2 T'_{lm}}{r'^3}\right]}$$

$$-\frac{r_i r_j}{r^2}\delta_{lm}\overline{\left[\frac{\ddot{T}_{ij}}{c_\infty^2 r} + \frac{3(1-M_\infty^2)\dot{T}_{ij}}{c_\infty r^2} + \frac{3(1-M_\infty^2)^2 T_{ij}}{r^3}\right]\left[\frac{\dot{T}'_{lm}}{c_\infty r'^2} + \frac{(1-M_\infty^2)T'_{lm}}{r'^3}\right]}$$

$$+\frac{2r_i r_j}{r^2}\frac{M_{\infty,l}M_{\infty,m}}{r'^3}\overline{\left[\frac{\ddot{T}_{ij}}{c_\infty^2 r} + \frac{3(1-M_\infty^2)\dot{T}_{ij}}{c_\infty r^2} + \frac{3(1-M_\infty^2)^2 T_{ij}}{r^3}\right]T'_{lm}}$$

Other terms are similar

Cross-Spectral Acoustic Analogy

$$G(\boldsymbol{x}_1, \boldsymbol{x}_2, \omega) = \frac{1}{16\pi^2} \int_{-\infty}^{\infty} \cdots \int_{-\infty}^{\infty} \left\{ \overbrace{F_t \overline{\ddot{T}_{ij} \ddot{T}'_{lm}}}^{\text{Far-Field Term}} + \overbrace{M_t \overline{\dot{T}_{ij} \dot{T}'_{lm}}}^{\text{Mid-Field Term}} + \overbrace{N_t \overline{T_{ij} T'_{lm}}}^{\text{Near-Field Term}} \right\}$$
$$\times \exp\left[-i\omega \left(\tau + \frac{|\boldsymbol{x}_1 - \boldsymbol{y}_1|}{c_\infty} - \frac{|\boldsymbol{x}_2 - \boldsymbol{y}_2|}{c_\infty} \right) \right] d\tau \, d\boldsymbol{\eta}' \, d\boldsymbol{\eta}$$

where the far-field term is, $F_t = \frac{r_i r_j r'_l r'_m}{r^2 r'^2} \left[\frac{1}{c_\infty^4 r r'} \right]$

and the mid-field term is,

$$M_t = \frac{r_i r_j r'_l r'_m}{r^2 r'^2} \left[\frac{9(1 - M_\infty^2)^2}{c_\infty^2 r^2 r'^2} - \frac{3(1 - M_\infty^2)^2}{c_\infty^2 r r'^3} - \frac{3(1 - M_\infty^2)^2}{c_\infty^2 r^3 r'} \right]$$
$$- \frac{r_i r_j r'_l}{r^2 r'} \left[\frac{6(1 - M_\infty^2)}{c_\infty^2} \left(\frac{2M_{\infty,m}}{r^2 r'^2} - \frac{M_{\infty,m}}{r r'^3} \right) \right] - \frac{r_i r'_l r'_m}{r r'^2} \left[\frac{6(1 - M_\infty^2)}{c_\infty^2} \left(\frac{2M_{\infty,j}}{r^2 r'^2} - \frac{M_{\infty,j}}{r^3 r'} \right) \right]$$
$$- \frac{r_i r_j}{r^2} \left[\frac{3(1 - M_\infty^2)\delta_{lm}}{c_\infty^2 r^2 r'^2} + \frac{(1 - M_\infty^2)\delta_{lm}}{c_\infty^2 r r'^3} + \frac{2M_{\infty,l} M_{\infty,m}}{c_\infty^2 r r'^3} \right]$$
$$- \frac{r'_l r'_m}{r'^2} \left[\frac{3(1 - M_\infty^2)\delta_{ij}}{c_\infty^2 r^2 r'^2} + \frac{(1 - M_\infty^2)\delta_{ij}}{c_\infty^2 r^3 r'} + \frac{2M_{\infty,i} M_{\infty,j}}{c_\infty^2 r^3 r'} \right]$$
$$+ \frac{r_i r'_l}{r r'} \left[\frac{16 M_{\infty,j} M_{\infty,m}}{c_\infty^2 r^2 r'^2} \right] + \frac{r_i}{r} \left[\frac{4M_{\infty,j}\delta_{lm}}{c_\infty^2 r^2 r'^2} \right] + \frac{r'_l}{r'} \left[\frac{4M_{\infty,m}\delta_{ij}}{c_\infty^2 r^2 r'^2} \right] + \frac{\delta_{ij}\delta_{lm}}{c_\infty^2 r^2 r'^2}$$

Miller, S. A. E., "Prediction of Near-Field Jet Cross Spectra,"
AIAA Journal, 2015. doi:10.2514/1.J053614.

Source Modeling

Two point correlation is modeled as

$$\overline{\ddot{T}_{ij}\ddot{T}'_{lm}} = \frac{\partial^4}{\partial \tau^4} R^v_{ijlm}(\boldsymbol{y}_1, \boldsymbol{\eta}, \tau)$$

For broadband shock-associated noise a great choice is

$$R^v_{ijlm} = k \frac{A_{ijlm}}{\pi^{1/2}\tau_s^4\omega^4} \frac{p_s p_{s,\eta}}{c^2} R_{ijlm}$$

That is compatible with previous modeling efforts

$$R_{ijlm} = \exp\left[\frac{-|\xi|}{\overline{u}\tau_s}\right] \exp\left[\frac{-(\xi - \overline{u}\tau)^2}{l_s^2}\right] \exp\left[\frac{-\eta^2}{l_{sy}^2}\right] \exp\left[\frac{-\zeta^2}{l_{sz}^2}\right]$$

Equivalent source model and cross-spectral acoustic analogy requires multiple integrations with retarded time. One is

$$\int\limits_{-\infty}^{\infty} \frac{\partial^4}{\partial \tau^4} \left\{ \frac{A_{ijlm}}{\pi^{1/2}\tau_s^4\omega^4} \frac{p_s p_{s,\eta} k}{c^2} \exp\left[\frac{-|\xi|}{\overline{u}\tau_s}\right] \exp\left[\frac{-(\xi - \overline{u}\tau)^2}{l_s^2}\right] \exp\left[\frac{-\eta^2}{l_{sy}^2}\right] \exp\left[\frac{-\zeta^2}{l_{sz}^2}\right] \right\} \exp\left[-i\omega\tau\right] d\tau$$

$$= \frac{A_{ijlm}}{\tau_s^4} \frac{p_s p_{s,\eta} k}{c^2} \frac{l_s}{\overline{u}} \exp\left[\frac{-|\xi|}{\overline{u}\tau_s}\right] \exp\left[\frac{-\eta^2}{l_{sy}^2}\right] \exp\left[\frac{-\zeta^2}{l_{sz}^2}\right] \exp\left[-\frac{\omega\left(4i\overline{u}\xi + l_s^2\omega\right)}{4\overline{u}^2}\right].$$

Double spatial integrals performed analytically in cylindrical coordinates
Note sources are located at relatively discrete locations

Cross-Spectrum of BBSAN Model Equation

The resulting model equation for the cross-spectrum of BBSAN is

$$
\boxed{
\begin{aligned}
G\left(\boldsymbol{x}_1, \boldsymbol{x}_2, \omega\right) = \frac{S_x^2 S_r^2}{4 c_\infty^4} \sum_{m=1}^{N_s} \sum_{n=1}^{N_s} \frac{A_{ijlm} p_{s,m} p_{s,n} k l_s z_m z_n}{\overline{c}^2 \overline{u} \tau_s^4 r_1^2 r_2^2} \exp\left[\frac{-l_s^2 \omega^2}{4\overline{u}^2}\right] \\
\times \exp\left[\frac{-4i\overline{u}(y_2 - y_1)\omega}{4\overline{u}^2}\right] \exp\left[\frac{-|y_2 - y_1|}{\overline{u}\tau_s}\right] \exp\left[\frac{-(z_m^2 + z_n^2)}{l_{sr}^2}\right] \\
\times \exp\left[-i\omega\left(\frac{|\boldsymbol{x}_1 - \boldsymbol{y}_1|}{c_\infty} - \frac{|\boldsymbol{x}_2 - \boldsymbol{y}_2|}{c_\infty}\right)\right] I_0\left(\frac{2 r_m r_n}{l_{sr}^2}\right)
\end{aligned}
}
$$

Descriptions of terms

Cross-Power Spectral Density

Double summation over shock wave shear layer positions, N_s

Grouped equivalent source term

Exponential equivalent source terms

Modified Bessel function of the first kind

Note if $\boldsymbol{x}_1 = \boldsymbol{x}_2$ then evaluation guarantees power-spectral density

Results

Far-Field Auto-Spectra

- Predictions of BBSAN auto-spectra
- Far-field at $R/D = 100$
- Observers on arc
- $M_d = 1.00$
- $M_j = 1.24$
- TTR = 1.00
- D = 0.0508 m

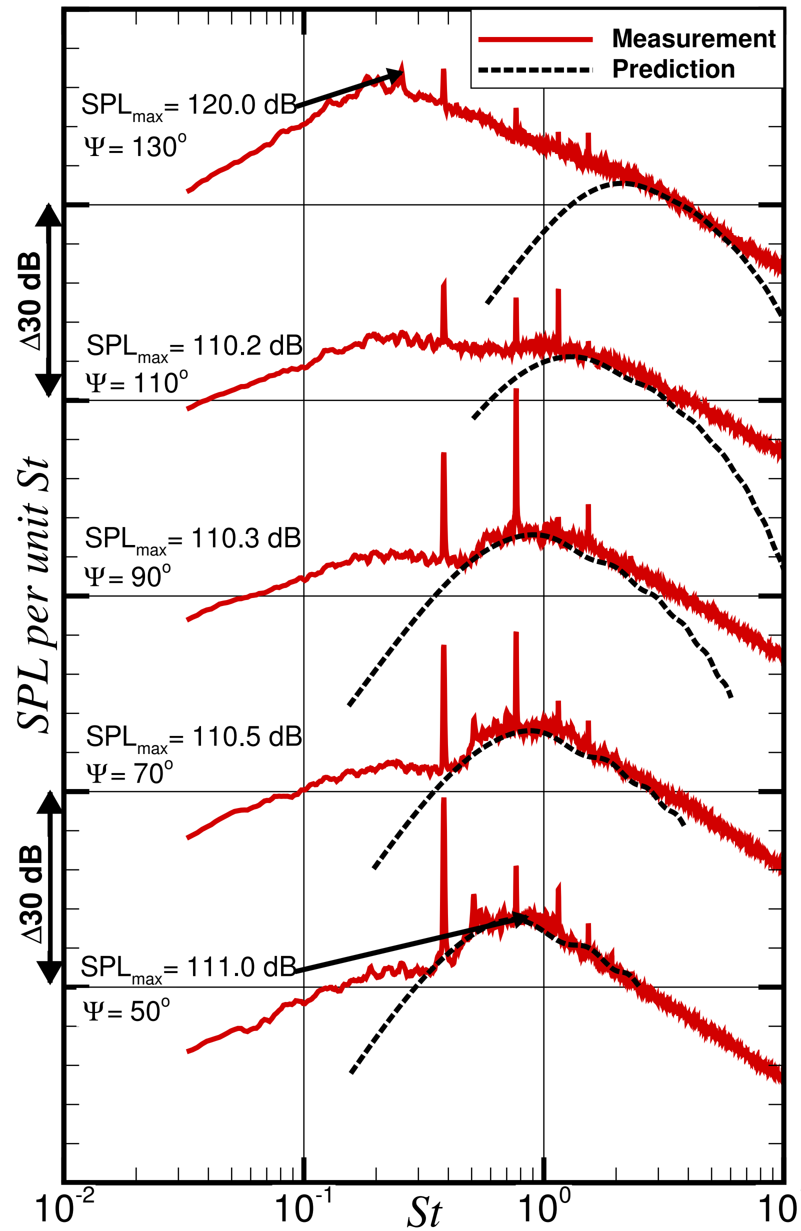

Measurements of, **Bridges, J. and Brown, C. A.**, `Validation of the Small Hot Jet Acoustic Rig for Aeroacoustic Research,' 11th AIAA/CEAS Aeroacoustics Conference, AIAA Paper 2005-2846, 2005. doi:10.2514/6.2005-2846.

Far-Field Auto-Spectra

$M_d = 1.00$, $M_j = 1.57$, TTR = 3.20

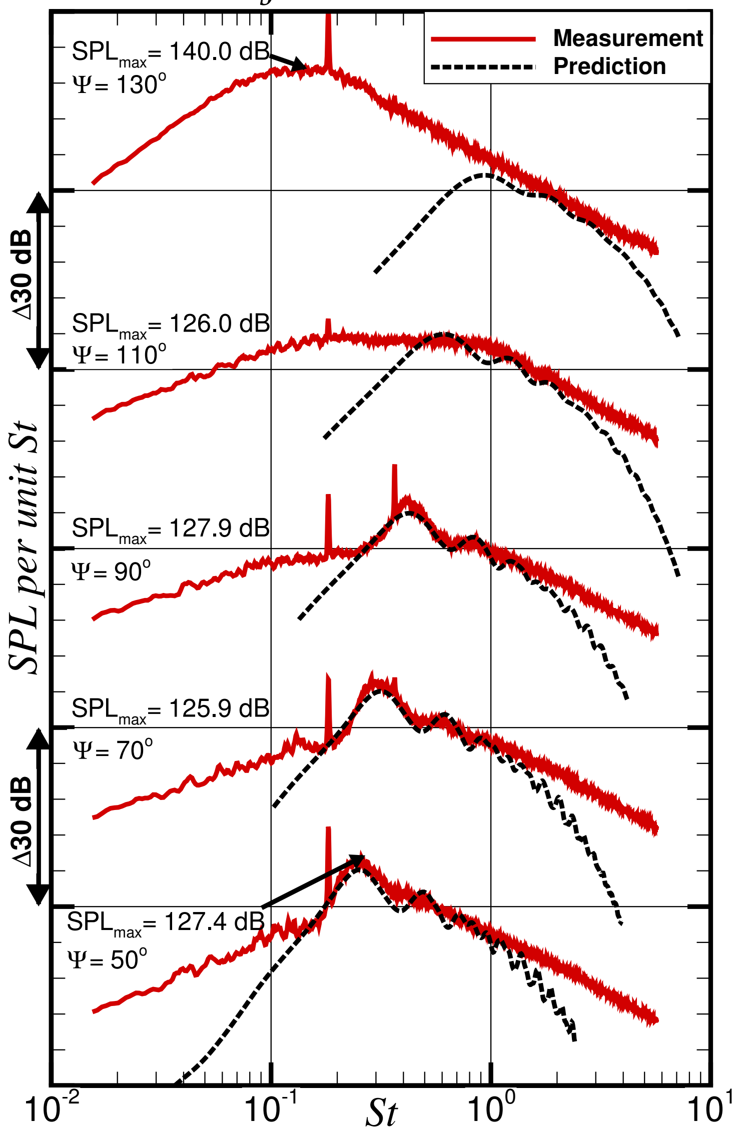

$M_d = 1.50$, $M_j = 1.294$, TTR = 1.00

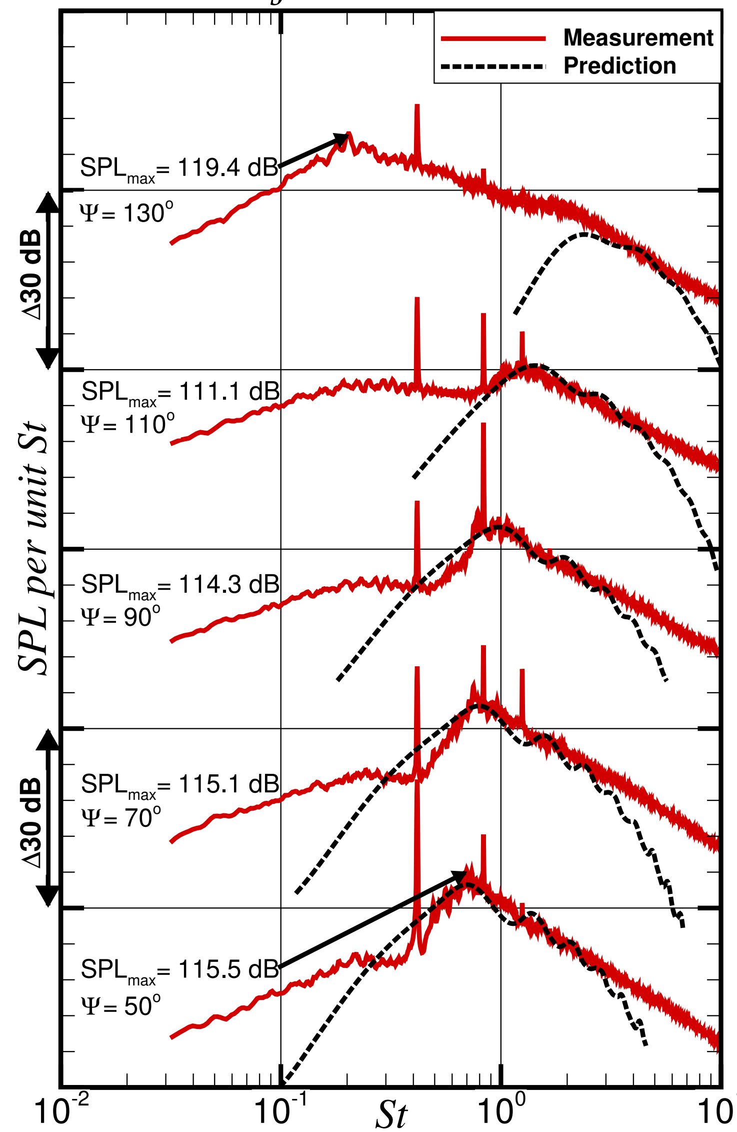

Near-Field Auto-Spectral Contours

Contours of SPL at $St = 1.86$ (16 kHz) from $M_d = 1.50$, $M_j = 1.67$, and TTR = 1.00 jet

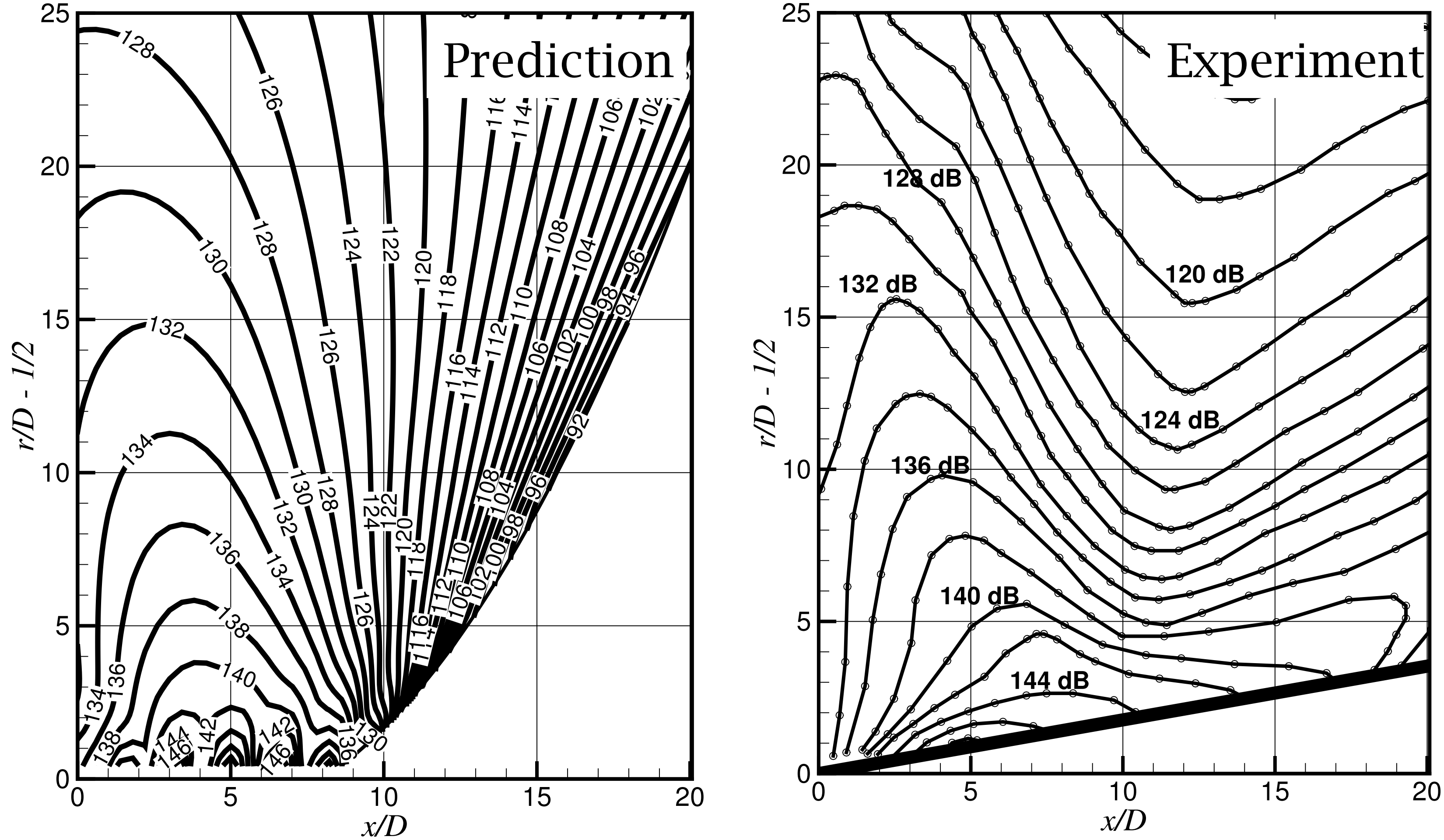

Measurements of, **Yu, J. C.**, `Investigation of the Noise Fields of Supersonic Axisymmetric Jet Flows,' Ph.D. Thesis, Syracuse University, 1971.

Near-Field Auto-Spectral Contours

Contours of SPL at $St = 4.67$ (40 kHz) from $M_d = 1.50$, $M_j = 1.67$, and TTR = 1.00 jet

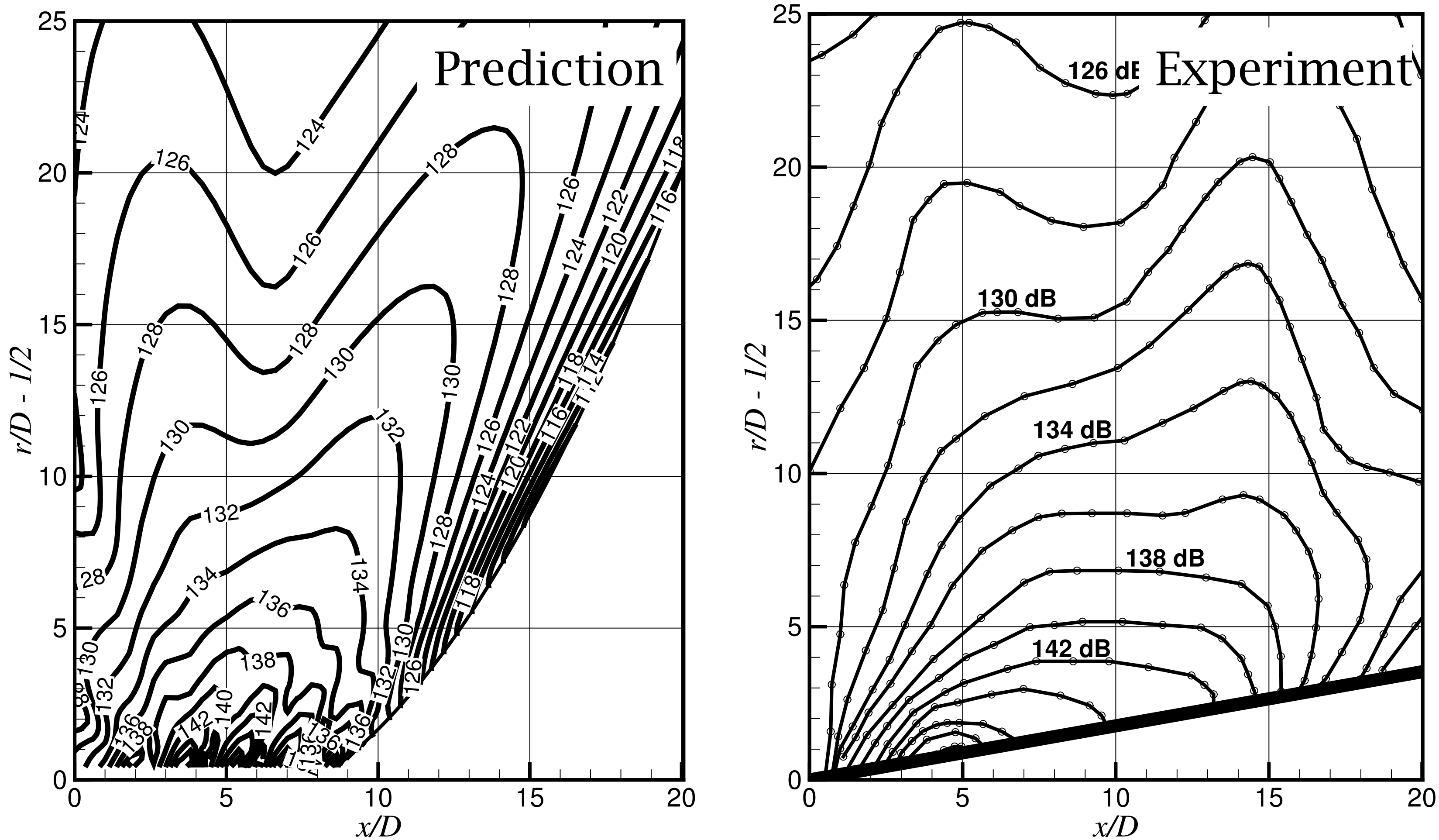

Measurements of, **Yu, J. C.**, `Investigation of the Noise Fields of Supersonic Axisymmetric Jet Flows,' Ph.D. Thesis, Syracuse University, 1971.

Near-Field Auto-Spectral Contours – Predictions Only

Contours of SPL from $M_d = 1.50$, $M_j = 1.67$, and TTR = 1.00 jet

Near-field detail showing coalescence of BBSAN radiation

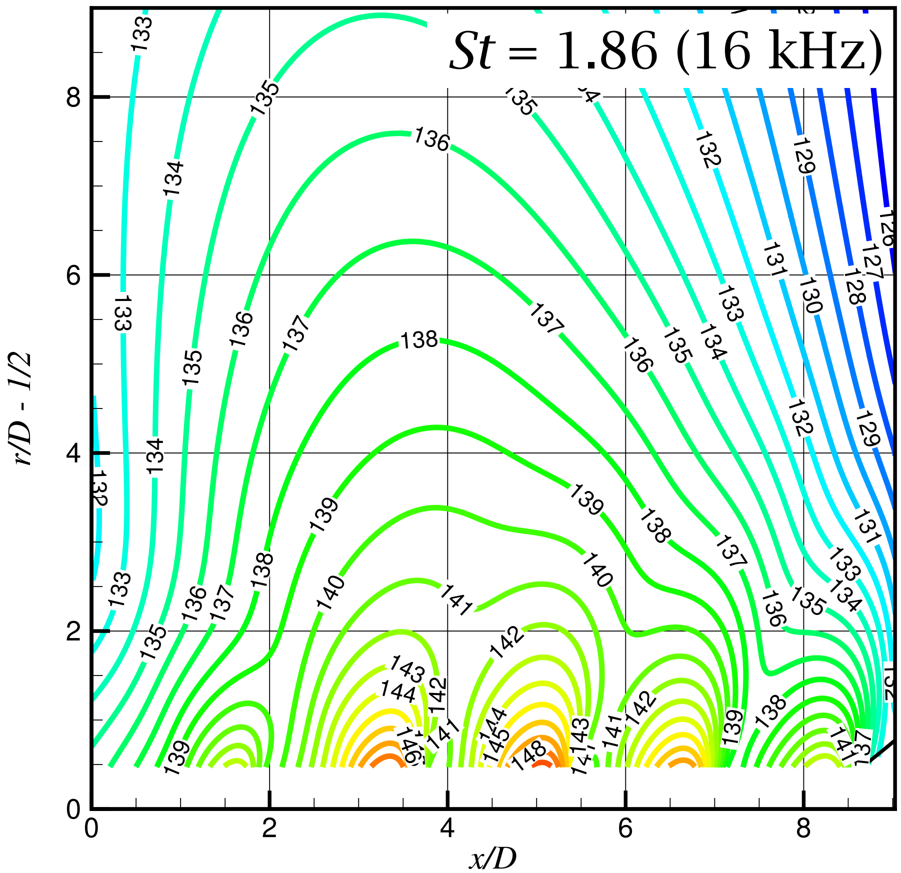

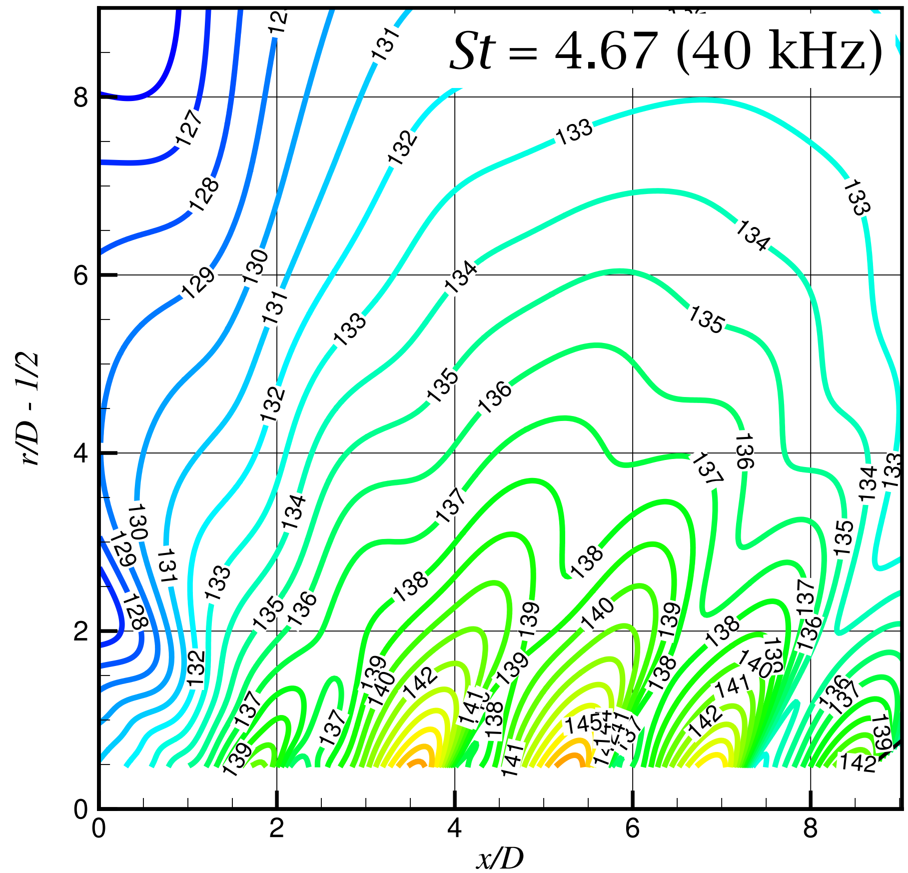

Far-Field Coherence

- Predictions of BBSAN coherence
- Far-field at $R/D = 100$
- Observers at sideline
- Observer pairs vary azimuthally
- $M_d = 1.00$
- $M_j = 1.24$
- TTR = 3.20

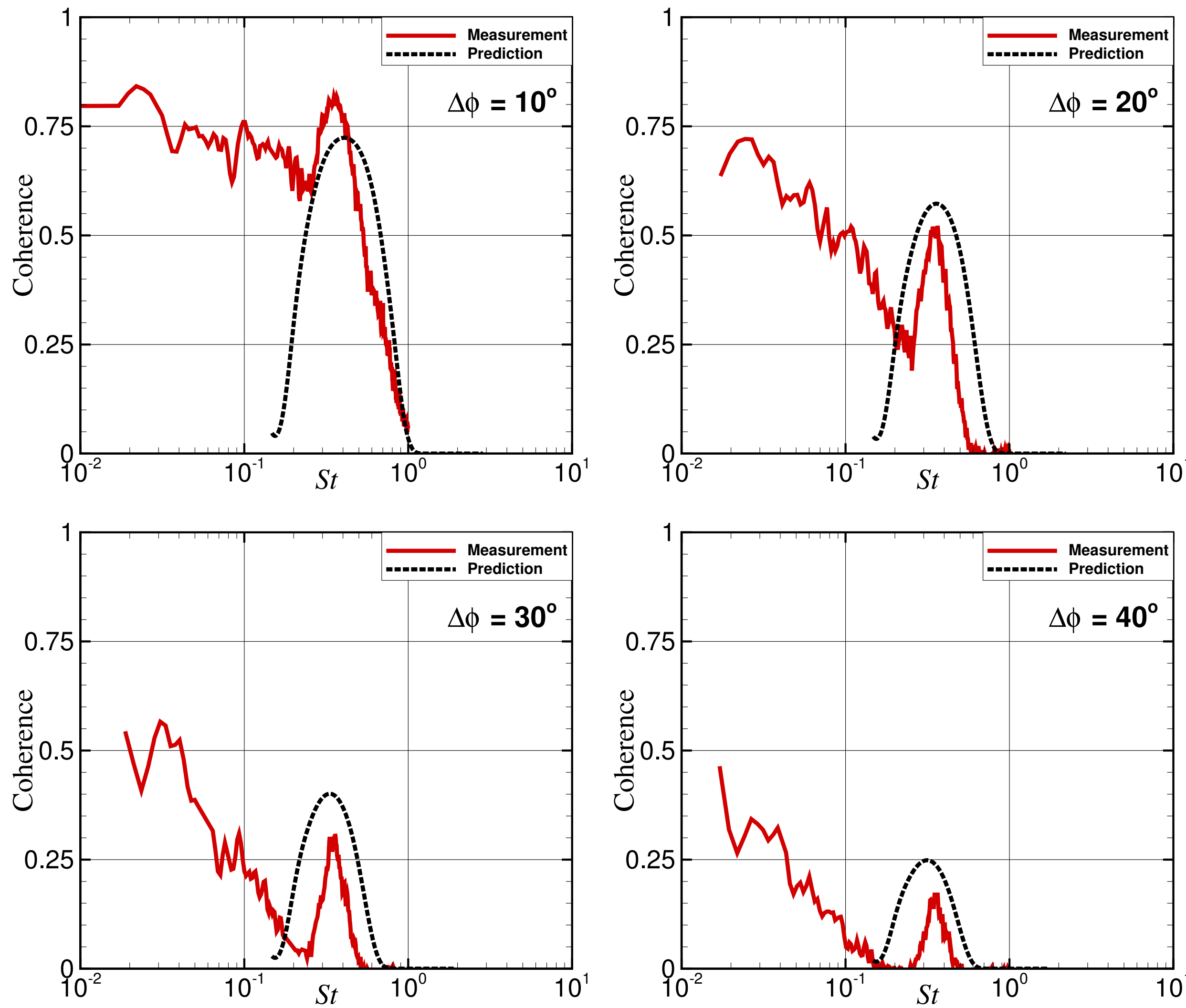

Measurements of, **Viswanathan, K., Alkislar, M. B., and Czech, M. J.,** `Characteristics of the Shock Noise Component of Jet Noise,' AIAA Journal, Vol. 48, No. 1, 2010, pp. 25–46. doi:10.2514/1.38521.

Far-Field Coherence

- Predictions of BBSAN coherence
- Far-field at $R/D = 100$
- Observers at sideline
- Observer pairs vary azimuthally
- $M_d = 1.00$
- $M_j = 1.57$
- TTR = 3.20

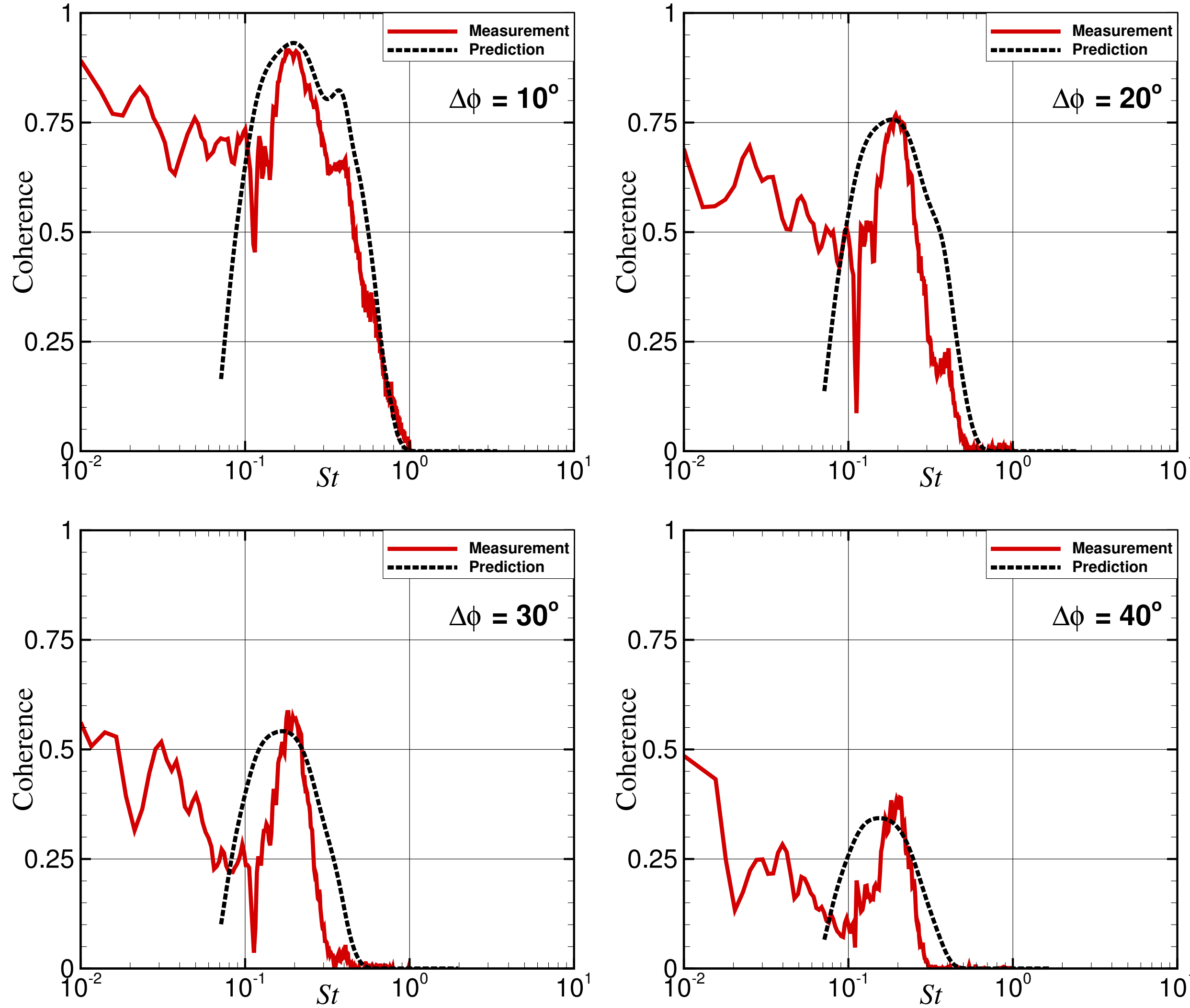

Measurements of, **Viswanathan, K., Alkislar, M. B., and Czech, M. J.**, `Characteristics of the Shock Noise Component of Jet Noise,' AIAA Journal, Vol. 48, No. 1, 2010, pp. 25–46. doi:10.2514/1.38521.

Near-Field Coherence

- Predictions of BBSAN coherence
- Near-field at $R/D = 4$
- Reference observer at sideline
- Observer pairs on linear array and vary axially
- $M_d = 1.00$
- $M_j = 1.16$
- TTR = 1.00

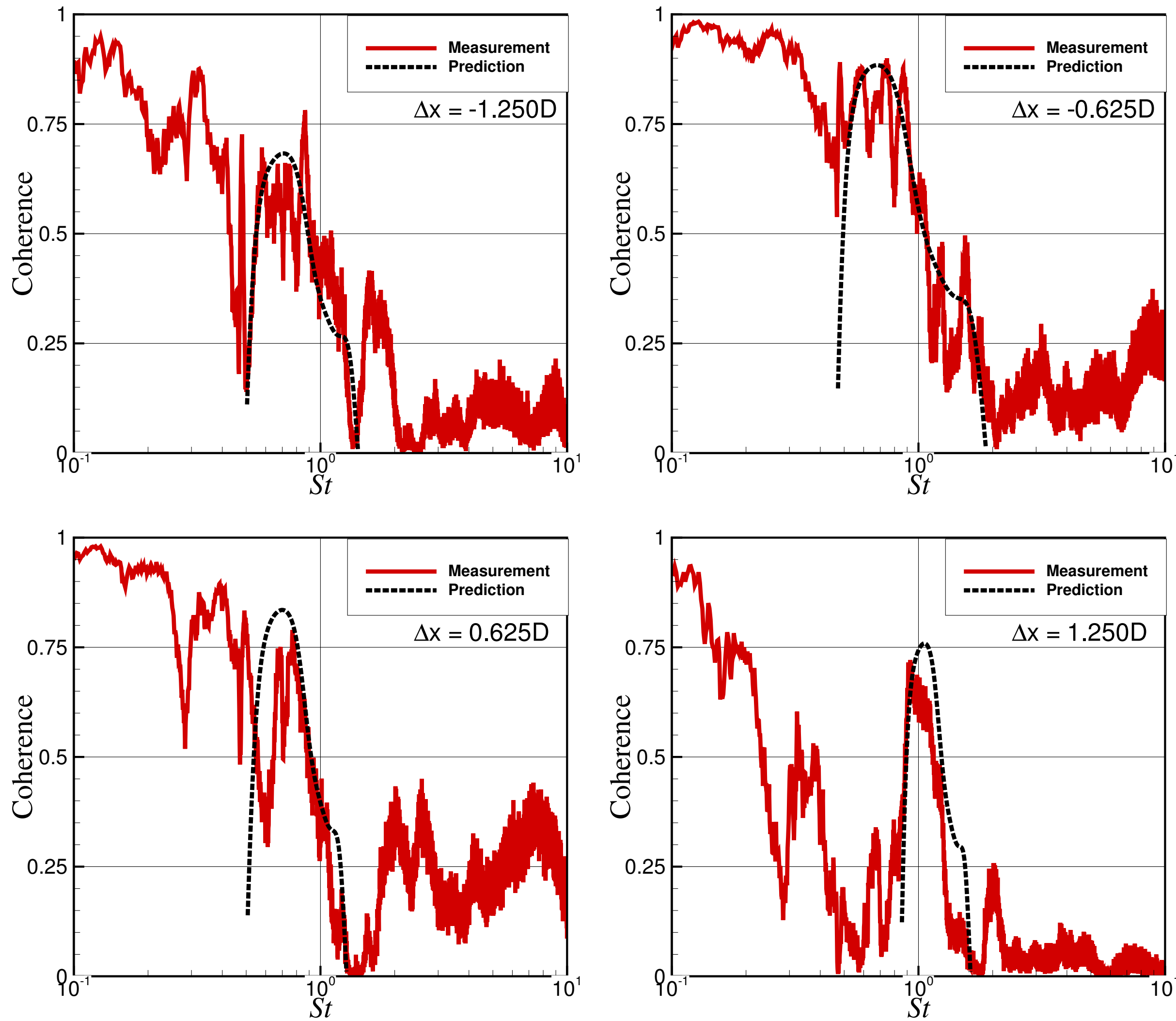

Measurements of, **Savarese, A., Jordan, P., Royer, A., Fourment, C., Collin, E., Gervais, Y., and Porta, M.,** `Experimental Study of Shock- Cell Noise in Underexpanded Supersonic Jets,' 19th AIAA/CEAS Aeroacoustics Conference, AIAA Paper 2013-2080, 2013. doi:10.2514/6.2013-2080.

Near-Field Coherence

- Predictions of BBSAN coherence
- Near-field at $R/D = 4$
- Reference observer at sideline
- Observer pairs on linear array and vary axially
- $M_d = 1.00$
- $M_j = 1.28$
- TTR = 1.00

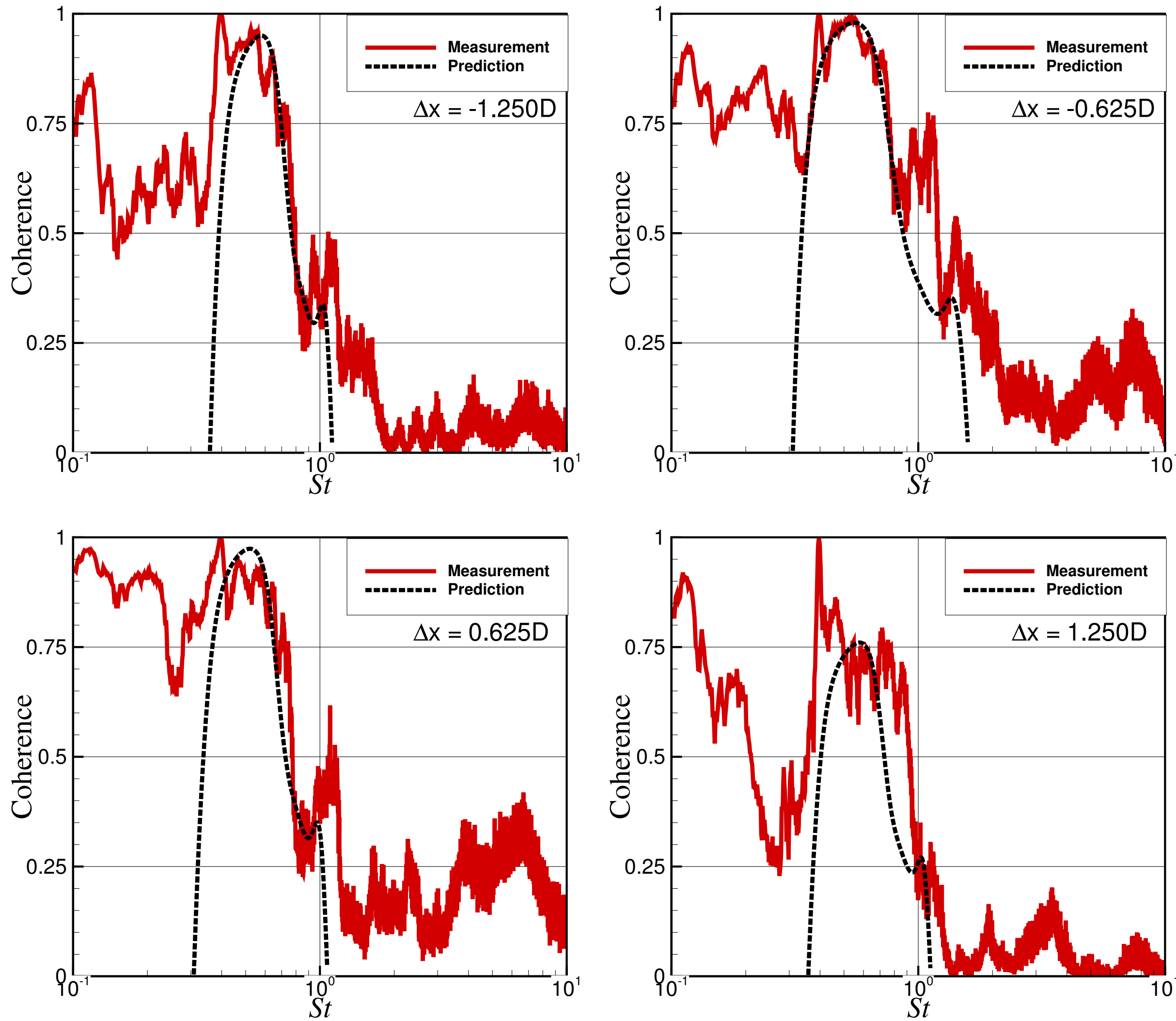

Measurements of, **Savarese, A., Jordan, P., Royer, A., Fourment, C., Collin, E., Gervais, Y., and Porta, M.,** `Experimental Study of Shock- Cell Noise in Underexpanded Supersonic Jets,' 19th AIAA/CEAS Aeroacoustics Conference, AIAA Paper 2013-2080, 2013. doi:10.2514/6.2013-2080.

Summary and Conclusion

- Formed equation for near-field BBSAN cross-spectra using cross-spectral acoustic analogy
- Equivalent source term captures physics and consistent with other models
- Validated near- and far-field, auto-spectra and coherence, with measurements
- Near-field auto-spectra show formation of increasing numbers of directional lobes
- Large variations observed in source intensity at each shock wave shear layer interaction
- Large broad lobes of coherence due to sound radiation from shock wave shear layer interactions, at lower and higher frequencies are due to other effects

Questions